Proteomics
Proteomics and Systems Biology

RESEARCH ARTICLE

Single polypeptide detection using a translocon EXP2 nanopore

Mitsuki Miyagi | **Sotaro Takiguchi** | **Kazuaki Hakamada** | **Masafumi Yohda** | **Ryuji Kawano**

Department of Biotechnology and Life Science, Tokyo University of Agriculture and Technology, Koganei-shi, Tokyo, Japan

Correspondence
Ryuji Kawano, Department of Biotechnology and Life Science, Tokyo University of Agriculture and Technology, Koganei-shi, Tokyo 184–8588, Japan.
Email: rjkawano@cc.tuat.ac.jp

Mitsuki Miyagi and Sotaro Takiguchi contributed equally to this work.

Abstract

DNA sequencing using nanopores has already been achieved and commercialized; the next step in advancing nanopore technology is towards protein sequencing. Although trials have been reported for discriminating the 20 amino acids using biological nanopores and short peptide carriers, it remains challenging. The size compatibility between nanopores and peptides is one of the issues to be addressed. Therefore, exploring biological nanopores that are suitable for peptide sensing is key in achieving amino acid sequence determination. Here, we focus on EXP2, the transmembrane protein of a translocon from malaria parasites, and describe its pore-forming properties in the lipid bilayer. EXP2 mainly formed a nanopore with a diameter of 2.5 nm assembled from 7 monomers. Using the EXP2 nanopore allowed us to detect poly-L-lysine (PLL) at a single-molecule level. Furthermore, the EXP2 nanopore has sufficient resolution to distinguish the difference in molecular weight between two individual PLL, long PLL (Mw: 30,000–70,000) and short PLL (Mw: 10,000). Our results contribute to the accumulation of information for peptide-detectable nanopores.

KEYWORDS
lipid bilayer, microfluidics, nanopore, peptide sensing, translocon

1 | INTRODUCTION

Nanopore technology is an emerging tool with great potential for single-molecule sensing. When a molecule enters a nanopore under an applied voltage, it can be recognized as an ionic current blockage, allowing for the detection of individual molecules with high sensitivity [1–7]. As a commercialized application of this technology, nanopore-based DNA sequencing has already been achieved by identifying the four individual nucleobases [8, 9]. The current challenge is the application of nanopore technology to peptide and protein sequencing.

Peptides and proteins are built from 20 kinds of amino acids, while DNA is comprised of four types of nucleic acids. The principle of electrical recognition of individual amino acids is the same as that of nucleic acids, but the detection of 20 distinguishable signals is a tremendous challenge. Using various pore-forming proteins shown in Table 1, some trials were reported for identifying the tiny structural difference of peptides from the constituted amino acids [10]. α-Hemolysin (αHL) nanopores [11], a popular biological nanopore for oligonucleotides

sensing, have also been used for peptide sensing [12–19]. Regarding peptide detection using the αHL pore, it has been shown that equipping αHL nanopores with $Au_{25}(SG)_{18}$ clusters can improve the mass resolution up to two-fold by increasing the on/off rate of peptides to the nanopore [20]. Fragaceatoxin C (FraC) nanopores [21] have recently enabled the discrimination of a 1.3 kDa difference in peptides by using a model biomarker [22]. Huang et al. successfully improved this resolution down to 44 Da by using variant FraC that had a smaller-sized constriction [23]. Aerolysin (AeL) nanopores [24, 25] have also been employed for the structural discrimination of peptides. A series of peptides with different charges and lengths [26] and with the same amino acid composition but different sequences [27] were both discriminated by using AeL nanopores. In terms of the length of peptides, it has been shown that AeL nanopores could resolve the signal of poly-arginine with a length ranging from 10 to 5 amino acids, with the resolution of one arginine [28]. Regarding the identification of single amino acids, AeL nanopores succeeded in distinguishing 13 of the 20 natural amino acids by using polycationic carriers [29]. Besides the above studies,

several kinds of biological nanopores have been used for peptide detection [30–34]. Nevertheless, it is still difficult to discriminate between individual amino acids whose size ranges less than 1 nm [35, 36]. This size is generally smaller than pore size, indicating that the size-matching between the pore diameter and the amino acid is one of the key requirements for discriminating between the 20 amino acids.
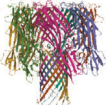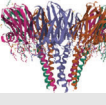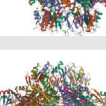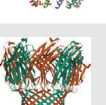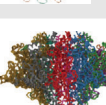
EXP2 is the transmembrane protein of a translocon from the malaria parasite *Plasmodium falciparum* [37] (Figure 1A,B). We have focused on EXP2 as the peptide-detectable nanopore because a translocon can transport a protein chain with unthreaded through the pore. The translocon called PTEX supports the malaria parasites to proliferate in human red blood cells by exporting proteins [38]. PTEX is composed of five proteins; EXP2 constitutes the transmembrane pore (Figure S1), while the other components play a role in unfolding the luggage proteins. Therefore, we consider EXP2 to have a suitable pore size for translocating an unfolded polypeptide. We have previously reported that the EXP2 formed a nanopore in a lipid bilayer without the other translocon components [39]. Here, we evaluate its pore-forming properties and apply it in single-molecule detection to investigate its capability for peptide sensing. Through our investigations, we reveal that EXP2 mainly forms a nanopore of 2.5 nm diameter, assembled from 7 monomers. Using the EXP2 nanopore, we were successful in detecting

poly-L-lysine (PLL) at a single-molecule level, and in size-discriminating between two individual PLL; long PLL (L-PLL, Mw: 30,000–70,000) and short PLL (S-PLL, Mw: 10,000).

Statement of significance

Nanopore technology has recently had attracted attention as the next generation of protein detection and amino acid sequencing. Finding an appropriate nanopore that is suitable for protein/peptide sensing is a key factor for realizing it. We here focus on EXP2, the transmembrane protein of a translocon from malaria parasites, and investigate its pore-forming properties and capability for peptide sensing. Through our experiments, we revealed that EXP2 mainly assembled from 7 monomers with a diameter of 2.5 nm in the lipid bilayer even without the other translocon components. Using the EXP2 nanopore, we were successful in detecting poly-L-lysine (PLL) at a single-molecule level, and in size-discriminating between long PLL (Mw: 30,000–70,000) and short PLL (Mw: 10,000). Our result will contribute to finding the appropriate nanopore of protein/peptide detection.

TABLE 1 Biological nanopores which have been used for peptide sensing

Nanopore	Diameter [nm][a]	Shape	Organism	PDBID	Ref.
α-hemolysin	1.4		*Staphylococcus aureus*	7AHL	[11-20, 35, 36]
FraC	1.6		*Actinia fragacea*	4TSY	[21–23]
Aerolysin	1.4		*Aeromonas hydrophila*	5JZT	[24–29]
Phi-29	3.6		*Bacillus* virus phi29	1H5W	[30]
SPP1	3.0		*Bacillus* phage SPP1	2JES	[31]
MspA	1.2		*Mycolicibacterium smegmatis*	1UUN	[32]
T7 connector	3.9		*Escherichia* phage T7	3J4A	[33, 34]

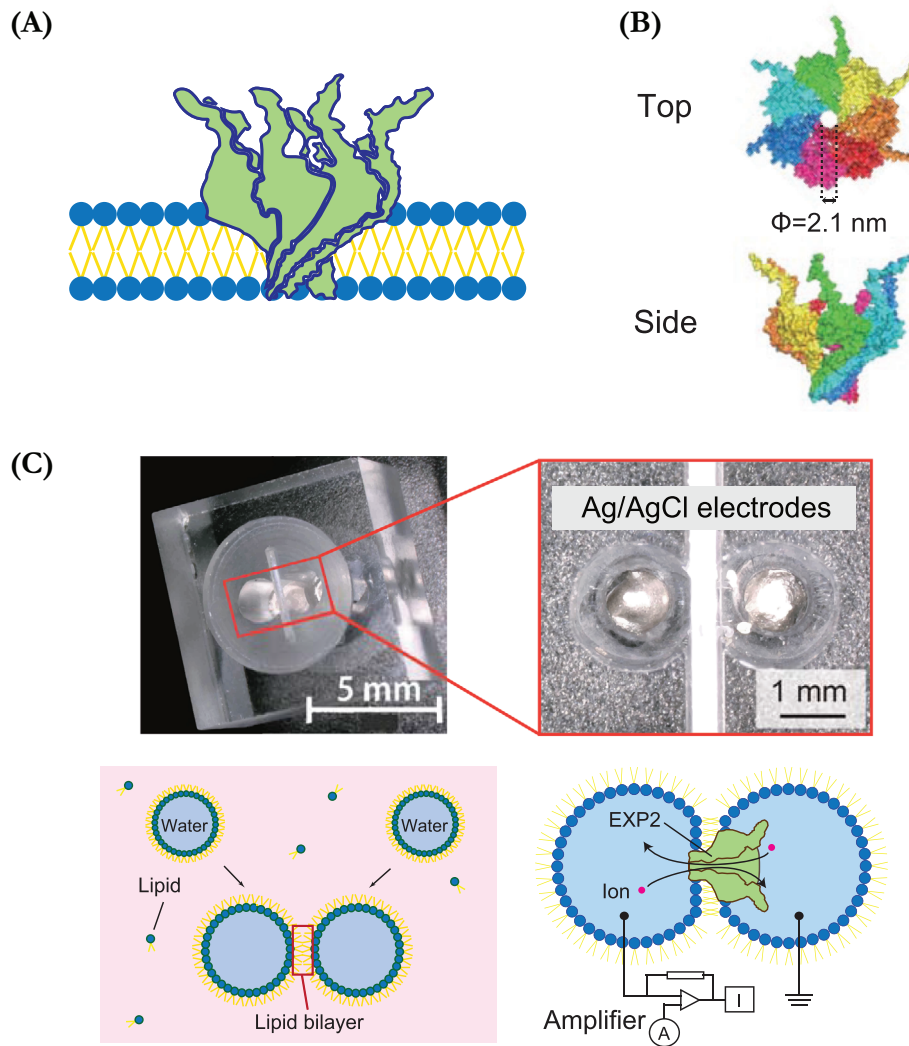[a]Diameter of the constriction region of nanopore.

FIGURE 1 (A) Illustration of an EXP2 nanopore reconstituted in a lipid bilayer. (B) The top and side view of the EXP2 nanopore (PDB ID: 6E10, previewed chains A-G by PyMOL). (C) Lipid bilayers are prepared by the droplet contact method using a microdevice, and the EXP2 nanopore is reconstituted in the lipid bilayer

2 | MATERIALS AND METHODS

2.1 | Regents and chemicals

The reagents used in this study were as follows: 1, 2-diphytanoyl-*sn*-glycero-3-phosphocholine (DPhPC; Avanti. Polar Lipids, Inc., USA), *n*-decane (Wako Pure Chemical Industries, Ltd., Japan), potassium chloride (KCl; Nacalai Tesque, Inc., Japan), 3-morpholinopropane-1-sulfonic acid (MOPS; Nacalai Tesque, Inc., Japan). Buffered electrolyte solutions (1 M KCl, 10 mM MOPS, pH 7.0) were prepared using ultrapure water, which was obtained from a Milli-Q system (Millipore, Billerica, MA, USA). Wild-type alpha-hemolysin (αHL; Sigma-Aldrich, St. Louis, MO, USA, and List Biological Laboratories, Campbell, CA, USA) was obtained as the monomer polypeptide, isolated from *Staphylococcus aureus* in the form of a powder and dissolved at a concentration of 1 mg/mL in ultrapure water. For use, samples were diluted to the designated concentration using a buffered electrolyte solution and stored

at 4°C. The 1 kbp double-stranded DNA (dsDNA), a part of lambda DNA (9346–10,345: 1 kbp), was purchased (Integrated DNA Technologies, Inc., USA), and the primers were synthesized by Fasmac Co., Ltd. (Kanagawa, Japan). KOD SYBR® qPCR Mix (TOYOBO Co., Ltd., Japan) and NucleoSpin Gel and PCR Clean-up (Takara Bio Inc., Japan) were used for the amplification of 1 kbp dsDNA. The long poly-L-lysine (Mw: 30,000–70,000, Sigma-Aldrich Japan, Inc., Japan) and short poly-L-lysine (Mw: 10,000, Alamanda-polymers, Inc., USA) were dissolved at a concentration of 1 mM and 5 mM in ultrapure water respectively, stored at –20 °C.

2.2 | Fabrication of the microdevice

The microdevice was fabricated by machining a 6.0 mm thick, 10 × 10 mm polymethyl methacrylate (PMMA) plate (Mitsubishi Rayon, Tokyo, Japan) using a computer-aided design and computer-aided

manufacturing with a three-dimensional modelling machine (MM-100, Modia Systems, Japan) as shown in Figure 1C. Two wells (2.0 mm diameter and 4.5 mm depth) and a chase between the wells were manufactured on the PMMA plate (Figure S2). Each well had a through-hole in the bottom and Ag/AgCl electrodes set into this hole (Figure 1C). A polymeric film made of parylene C (polychloro-*p*-xylylene) with a thickness of 5 μm as shown in Figure S2 was patterned with a single pore (100 μm diameter) using a conventional photolithography method and then fixed between PMMA films (0.2 mm thick) using an adhesive bond (Super X, Cemedine Co., Ltd., Tokyo, Japan). The films, including the parylene film, were inserted into the chase to separate the wells.

2.3 | Lipid bilayer preparation and reconstitution of the EXP2 nanopore

Lipid bilayers were prepared using the device produced by microfabrication (Figure 1C). Lipid bilayers can be simultaneously formed in this device by the droplet contact method (Figure 1C) [40, 41]. In this method, the two lipid monolayers contact each other and form lipid bilayers on a parylene C film that separates two chambers. Lipid bilayers were formed as follows: each chamber of the device was filled with *n*-decane (0.5 μL) containing the lipid composition of DPhPC (10 mg/mL). Wild-type EXP2 monomers were expressed by *E. coli* following our previous protocol [39] and were dissolved at a concentration of 760 nM in 20% glycerol, and stored at −80°C. The buffer solution (4.7 μL) containing EXP2 (final concentration 80 nM) was poured into one chamber which was connected to the ground terminal. The buffer solution (4.7 μL) without EXP2 was poured into another chamber which was connected to the recoding terminal (Figure 1C). In this study, the buffer solution was the same for both droplets (1 M KCl and 10 mM MOPS (pH 7.0)). Within a few minutes of adding the solutions, lipid bilayers formed and EXP2 created nanopores from the poured chamber by reconstitution in the lipid bilayers. If the lipid bilayers ruptured during this process, they were recreated by tracing at the interface of the droplet with a hydrophobic stick.

2.4 | Channel current measurement and data analysis

The channel current was monitored using an Axonpatch 200B amplifier (Molecular Devices, USA) or a Pico patch-clamp amplifier (Tecella, Foothill Ranch, CA, USA). The signals were detected using a 10 kHz low-pass Bessel filter at a sampling frequency of 50 kHz in Axonpatch 200B and an 8 kHz low-pass Bessel filter at a sampling frequency of 40 kHz in Pico patch-clamp. A constant voltage of + 100 mV was applied to the recording chamber, and the other chamber was grounded. The recorded data from Axonpatch 200B were acquired with Clampex 9.0 software (Molecular Devices, USA) through a Digidata 1440A analog-to-digital converter (Molecular Devices, USA). Data were analysed using Clampfit 11.1 (Molecular Devices, USA), Excel (Microsoft, Washington, USA), Origin pro 8.5J (Light Stone,

Tokyo, Japan), and python 3.5 (Python Software Foundation, USA). Channel current measurements were conducted at 22 ± 2°C.

Detection of double-stranded DNA. The ground side solution contained dsDNA and EXP2 (Figure S3). A constant voltage of + 100 mV was applied to the recording chamber.

Detection of poly-L-lysine. The recoding side solution contained poly-L-lysine and EXP2 (Figure S3). A constant voltage of + 100 mV was applied to the recording chamber.

Data analysis for single-molecule detection. The analysed data were obtained from at least three different EXP2 nanopores. We defined that dsDNA and poly-L-lysine were detected when > 0.5 nS of open EXP2 channel currents were inhibited. The duration time was filtered to < 1 ms to exclude distinctive signals from EXP2 (the detail is described in Figure S4). The bootstrap method is a method based on the resampling of the original random sample, drawn from a population with an unknown distribution. We used the exact bootstrap method, which availed of the entire space of resamples. In the exact bootstrap method, accuracy verification is possible when the sample number is over 30 [42]. In this study, our bootstrap procedure took 120 samples randomly from the primary common translocation data with 65,536 replacements and calculated the mean for these samples. Three hundred samples were randomly extracted from the bootstrapped data to produce the scatter plot of duration time versus current blocking conductance.

2.5 | Preparation of 1 kbp double-stranded DNA

1 kbp dsDNA, a part of lambda DNA (9346–10,345: 1 kbp), was purchased and amplified using PCR. First, 0.01 ng/mL template DNA (45 μL), and 10 μM each of either the forward or reverse primer (9 μL, respectively), and ultrapure water (162 μL) were mixed in a 1.5 mL DNA low-bind tube. Subsequently, 25 μL of each solution was poured into a PCR tube. The PCR reaction solution contained KOD SYBR qPCR Mix (half of the total volume, 25 μL). PCR was carried out using a Thermal Cycler to amplify the 1 kbp dsDNA by the following production steps: preheat at 98°C for 2 min; 40 cycles of 98°C for 10 s, 57°C for 10 s, 68°C for 1 min. Then, the amplified dsDNA was purified by NucleoSpin Gel and PCR Clean-up. The concentration of purified dsDNA was confirmed by the absorbance at 260 nm using the NanoDrop 2000c (Thermo Scientific).

3 | RESULTS AND DISCUSSION

3.1 | Current signal classification for the evaluation of pore-forming properties

The pore-forming properties of EXP2 were examined by channel current measurements using our lipid bilayer system (Figure 1C) [43–46]. As shown in Figure 2A,B, step-like signals and the other different shapes of current signals were observed under + 100 mV. Following our proposed current signal classification for the different signal shapes,
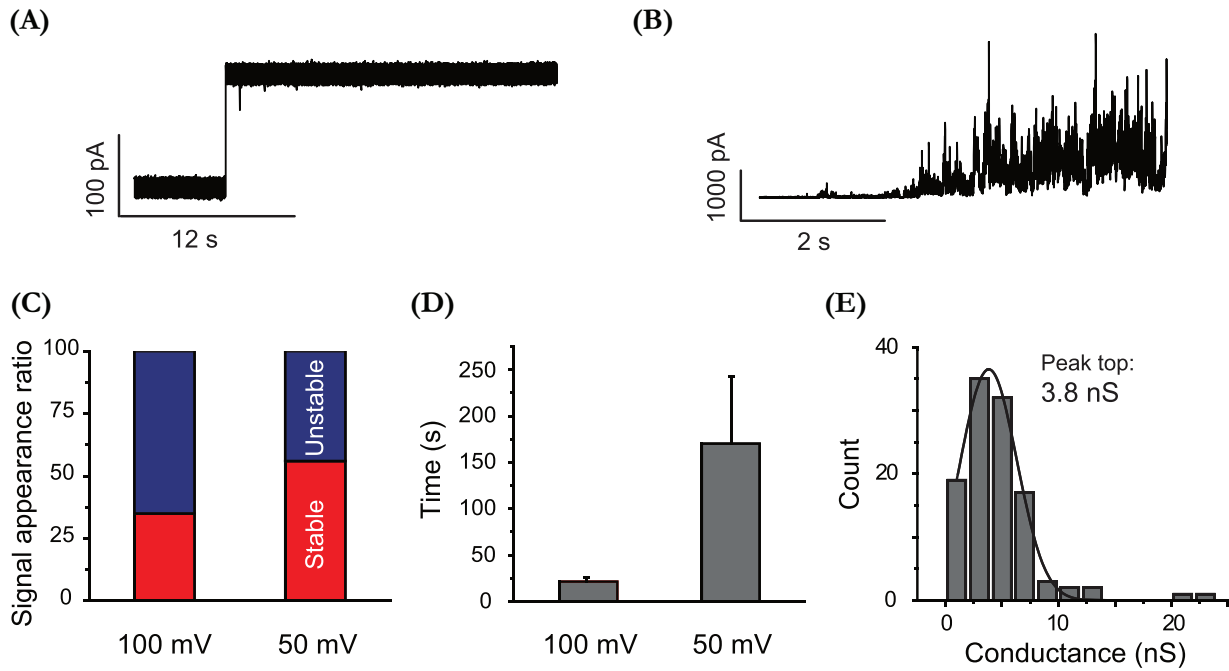
FIGURE 2 Typical current-time traces of EXP2 at + 100 mV, which are classified into (A) stable pore formation, and (B) unstable pore formation. (C) The ratio of stable and unstable pore formation, calculated from the channel current analysis. (D) The average of the lifetime, which is the length of time that the pore is open with a plateau current state. (E) Histogram of the current conductance for the initial step increase from the 0 A (baseline)

we classified the current signals into four types; step, square-top, multi-level, and erratic (Figure S5) [47–49]. The detailed definition of this signal classification is described in Figure S5. To evaluate the pore-forming activity of EXP2, we here defined step and square-top as signals relating to the formation of stable pores. Multi-level and erratic are considered to correlate with unstable pore formation. In the channel current measurements, the ratio of stable signals was 35% (Figure 2C). We have previously reported that the other pore-forming proteins showed a higher stable signal ratio, of at least around 60% [50]. Hence, optimization of the experimental conditions of the EXP2 nanopore is required in order to increase the formation of stable pores. As shown in Table S1, EXP2 has lots of charged amino acids, so we attempted to stabilize the nanopores by reducing the energy of the electric field. As predicted, the appearance ratio of stable signals increased to 56% when decreasing the applied voltage from + 100 to + 50 mV (Figure 2C, the detailed result of signal classification is shown in Figure S6). In terms of the lifetime, which is the time of the pore-opening plateau state (Figure S7), it was also improved by the optimization of the applied voltage, resulting in about eight-fold prolongation (Figure 2D).

3.2 | Analysis of the pore size and the number of assembled EXP2 monomers

Although cryo-electron microscopy observations showed the rigid structure of EXP2 as a part of the translocon [38], it is necessary to investigate the dynamic pore size of EXP2 in the lipid bilayer without the other translocon components. The size of the pore can be theoret-

ically calculated using the current conductance of the step signals and Hille's equation as follows:

$$R = \left(l + \frac{\pi r}{2}\right) \frac{\rho}{\pi r^2} \qquad (1)$$

Here, r is the pore radius, l is the pore length (13 nm for the EXP2), ρ is the solvent resistivity, and R is the resistance of the pore. R is calculated as V/I, where I is the current through the pore and V is the applied voltage between two chambers. The open channel conductance was defined as the amplitude of the initial step signals from the baseline. As shown in Figure 2E, the histogram of the pore conductance of EXP2 showed Gaussian distribution with a peak at 3.8 nS, which corresponds to a pore diameter of 2.5 nm.

Next, we mathematically estimated the number of assembled monomers from the step signals as follows [51]:

$$d = a\left(\frac{1}{\sin(\pi/n)} - 1\right) \qquad (2)$$

where d is the pore diameter, a is the width of the EXP2 monomer from the PDB (1.77 nm for EXP2, PDB ID: 6E10), and n is the number of assembled monomers [50]. With the substitution of calculated pore diameter for d, the assembling monomer number was calculated to be 7 monomers for the peak value of the histogram. Considering the wide distribution of the conductance, it may possible that the EXP2 formed polydisperse-sized nanopores assembled from 5 to 9 monomers, with the 7-mer nanopore most frequently observed. This result was consistent with the in vivo condition that the EXP2 nanopore is combined with other translocon components [38].
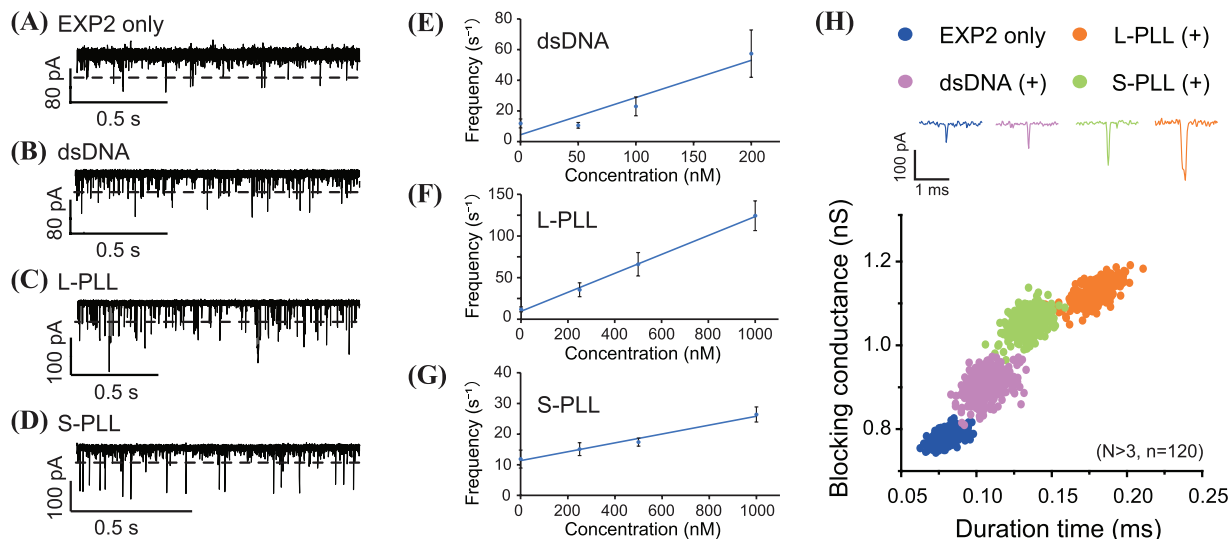
FIGURE 3 Results of the single-molecule detection using the EXP2 nanopore at the applied voltage of +100 mV. (A) The typical step signal of the EXP2 nanopore without any additional molecules. (B-D) The typical current-time traces of EXP2 with (b) dsDNA, (C) L-PLL, and (D) S-PLL at the concentration of 200 nM, 1μM, and 1 μM. (E-G) The event frequency as a function of the concentration of (E) dsDNA, (F) L-PLL, and (G) S-PLL. (H) Each typical blocking signal and the scatter plot of duration time versus current blocking conductance. The bootstrapped data were used to produce the scatter plot (N is the number of EXP2 nanopores and n is the number of blocking signals)

3.3 | Single-molecule detection using the EXP2 nanopore

The optimized + 50 mV was not suitable for the molecular detecting experiments (Figure S8), probably owing to the insufficient electrical force to get the target molecule captured into the nanopore, so we conducted the following experiments at + 100 mV. Single-stranded DNA is able to pass through conventional biological nanopores such as αHL and MspA [52, 53], whereas double-stranded DNA cannot pass and clogs the pore vestibules owing to the size mismatch between dsDNA and pore diameter. EXP2 mainly formed nanopores with a diameter of 2.5 nm, which is close to the diameter of dsDNA. Therefore, we first attempted to detect dsDNA with a length of 1 kbp using the EXP2 nanopore. In the channel current measurements, blocking signals that reflect the detection of dsDNA were observed at concentrations 50, 100, and 200 nM (Figure 3B), and the frequency of blocking events increased with an increase in dsDNA concentration (Figure 3E). Although EXP2 has noise-like signals in the pore-opening plateau states (Figure 3A), probably owing to the fluctuation of its C-terminus charged amino acids, the dsDNA detection signals could still be discriminated in the scatter plot of duration time versus blocking conductance (Figure 3H).

Next, we attempted to detect poly-L-lysine (PLL) to check the capability of EXP2 as a biological nanopore for polypeptide sensing. The channel current measurement was conducted using two individual PLL, long-PLL (L-PLL) with molecular weight ranging from 30,000 to 70,000, and short-PLL (S-PLL) with a molecular weight of 10,000. The blocking signals were observed at concentrations 250, 500, and 1000 nM of each PLL (Figure 3C,D), and the blocking frequency depended on the concentration of each molecule (Figure 3F,G). Depending on the difference of the total charge [54], L-PLL showed a larger frequency than

that of S-PLL. The scatter plot could distinguish the detection signals of each PLL from the EXP2 noise-like signals. PLL forms differing random-coil structures in aqueous solution depending on its length [55], resulting in different blocking conductance (Figure 3H). Regarding the duration time, it is considered to reflect the time for the target molecule to translocate through the nanopore. Thus, L-PLL showed a longer duration time than that of S-PLL owing to its molecular length. In other words, the EXP2 nanopore had the resolution to distinguish the difference in molecular weight between L-PLL and S-PLL.

We here compared the polypeptide sensing ability of EXP2 with αHL as a common biological nanopore for sensing applications. It is revealed that the frequency of the detection events through the EXP2 nanopore was higher than that of the αHL nanopore (Figure 4A-C) at the same 1 μM L-PLL. As shown in Figure 4D,E, the properties of the nanopores such as electrostatic potential mapping and shape are significantly different between EXP2 and αHL, resulting in the difference in event frequency.

4 | CONCLUSION

We examined the pore-forming properties of EXP2, the transmembrane protein of a translocon from a malaria parasite, through channel current measurements. The results reveal that EXP2 forms a nanopore mainly assembled from seven monomers with a diameter of 2.5 nm in the lipid bilayer. These data were consistent with in vivo conditions where EXP2 forms a nanopore with other translocon components. Using the EXP2 nanopore allowed us to detect dsDNA with a length of 1 kbp and PLL at a single-molecule level. Regarding polypeptide sensing, the EXP2 nanopore has the resolution to distinguish the difference of molecular weight between L-PLL (Mw: 30,000–70,000)
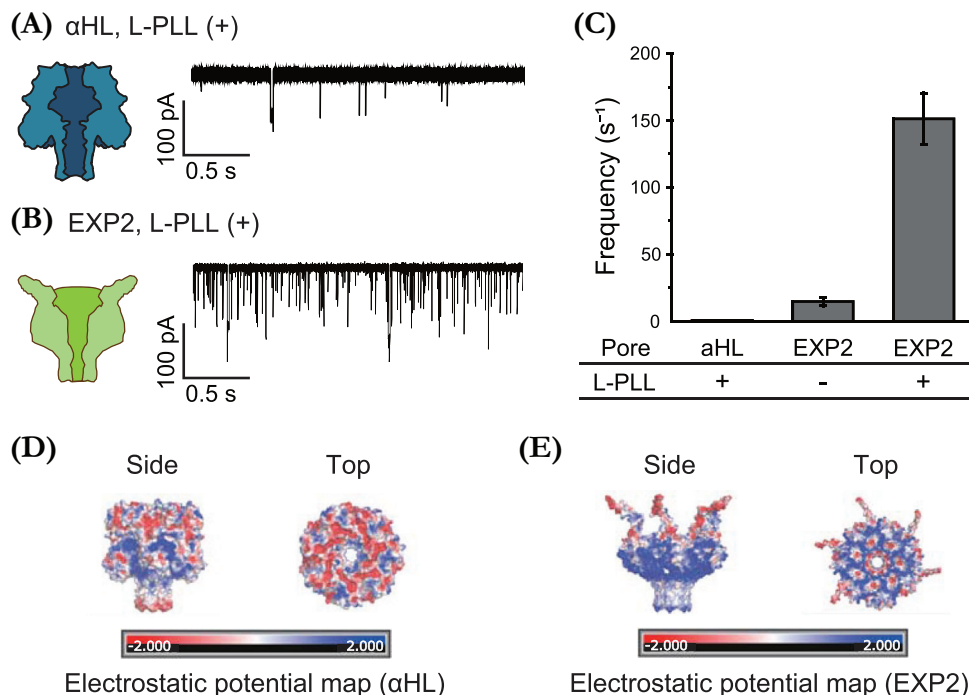
(A) αHL, L-PLL (+)

(B) EXP2, L-PLL (+)

(C)

(D) Side   Top

Electrostatic potential map (αHL)

(E) Side   Top

Electrostatic potential map (EXP2)

FIGURE 4 Typical detection signals of L-PLL at the concentration of 1 μM through (A) αHL and (B) EXP2 at + 100 mV. (C) Analysis of the frequency of the blocking signals reflecting the detection of L-PLL by each nanopore. The calculated frequency of 1 μM L-PLL detection was 0.86 ± 0.19 s^{-1} for αHL, and 151 ± 19 s^{-1} for EXP2. (D-E) The three dimensional model and the electrostatic potential map of (D) αHL nanopore and (E) EXP2 nanopore at neutral pH condition. The electrostatic potential was calculated through the APBS tool in PyMOL software.

and S-PLL (Mw: 10,000). Analysis of detection event frequency indicated that EXP2 is more suitable to detect polycationic peptides than the αHL nanopore. Nanopore sensing has recently been postulated as a promising technology in mass spectrometry [56], especially peptide mass analysis [23]. Our data supports the potential of the translocon nanopore in such chemical and biological sensing applications.

CONFLICT OF INTEREST

The authors declare no conflict of interest.

DATA AVAILABILITY STATEMENT

All data is included in this published article and its Supplementary Information file.

REFERENCES

1. Kasianowicz, J. J., Brandin, E., Branton, D., & Deamer, D. W. (1996). Characterization of individual polynucleotide molecules using a membrane channel. *Proceedings of the National Academy of Sciences of the United States of America*, *93*(24), 13770–13773.
2. Gu, L.-Q., Braha, O., Conlan, S., Cheley, S., & Bayley, H. (1999). Stochastic sensing of organic analytes by a pore-forming protein containing a molecular adapter. *Nature*, *398*, 686–690.
3. Reiner, J. E., Balijepalli, A., Robertson, J. W. F., Campbell, J., Suehle, J., & Kasianowicz, J. J. (2012). Disease detection and management via single nanopore-based sensors. *Chemical Reviews*, *112*(12), 6431–6451.
4. Stoloff, D. H., & Wanunu, M. (2013). Recent trends in nanopores for biotechnology. *Current Opinion in Biotechnology*, *24*(4), 699–704.
5. Cao, C., & Long, Y. T. (2018). Biological nanopores: Confined spaces for electrochemical single-molecule analysis. *Accounts of Chemical Research*, *51*(2), 331–341.
6. Kawano, R., (2018). Nanopore decoding of oligonucleotides in DNA computing. *Biotechnology Journal*, *13*(12), 1800091.
7. Ding, T., Yang, J., Pan, V., Zhao, N., Lu, Z., Ke, Y., & Zhang, C. (2020). DNA nanotechnology assisted nanopore-based analysis. *Nucleic Acids Research*, *48*(6), 2791–2806.
8. Branton, D., Deamer, D. W., Marziali, A., Bayley, H., Benner, S. A., Butler, T., Di Ventra, M., Garaj, S., Hibbs, A., Huang, X., Jovanovich, S. B., Krstic, P. S., Lindsay, S., Ling, X. S., Mastrangelo, C. H., Meller, A., Oliver, J. S., Pershin, Y. V., Ramsey, J. M., … Schloss, J. A. (2008). The potential and challenges of nanopore sequencing. *Nature Biotechnology*, *26*, 1146–1153.
9. Jain, M., Olsen, H. E., Paten, B., & Akeson, M. (2016). The Oxford nanopore MinION: Delivery of nanopore sequencing to the genomics community. *Genome Biology*, *17*, 239.
10. Oukhaled, A., Bacri, L., Pastoriza-Gallego, M., Betton, J. - M., & Pelta, J. (2012). Sensing proteins through nanopores: Fundamental to applications. *ACS Chemical Biology*, *7*(12), 1935–1949.
11. Song, L., Hobaugh, M. R., Shustak, C., Cheley, S., Bayley, H., & Gouaux, J. E. (1996). Structure of staphylococcal alpha-hemolysin, a heptameric transmembrane pore. *Science*, *274*(5294), 1859–1865.
12. Sutherland, T. C., Long, Y. T., Stefureac, R. I., Bediako-Amoa, I., Kraatz, H. B., & Lee, J. S. (2004). Structure of peptides investigated by nanopore analysis. *Nano Letters*, *4*(7), 1273–1277.

13. Stefureac, R., Long, Y. T., Kraatz, H. B., Howard, P., & Lee, J. S. (2006). Transport of α-helical peptides through α-hemolysin and aerolysin pores. *Biochemistry*, *45*(30), 9172–9179.

14. Asandei, A., Chinappi, M., Lee, J. K., Ho Seo, C., Mereuta, L., Park, Y., & Luchian, T. (2015). Placement of oppositely charged aminoacids at a polypeptide termini determines the voltage-controlled braking of polymer transport through nanometer-scale pores. *Scientific Reports*, *5*, 10419.

15. Asandei, A., Rossini, A. E., Chinappi, M., Park, Y., & Luchian, T. (2017). Protein nanopore-based discrimination between selected neutral amino acids from polypeptides. *Langmuir*, *33*(50), 14451–14459.

16. Movileanu, L., Schmittschmitt, J. P., Martin Scholtz, J., & Bayley, H. (2005). Interactions of peptides with a protein pore. *Biophysical Journal*, *89*(2), 1030–1045.

17. Mereuta, L., Asandei, A., Seo, C. H., Park, Y., & Luchian, T. (2014). Quantitative understanding of pH- and salt-mediated conformational folding of histidine-containing, beta-hairpin-like peptides, through single-molecule probing with protein nanopores. *ACS applied materials & interfaces*, *6*(15), 13242–13256.

18. Nivala, J., Marks, D. B., & Akeson, M. (2013). Unfoldase-mediated protein translocation through an α-hemolysin nanopore. *Nature Biotechnology*, *31*(3), 247–250.

19. Asandei, A., Schiopu, I., Chinappi, M., Seo, C. H., Park, Y., & Luchian, T. (2016). Electroosmotic trap against the electrophoretic force near a protein nanopore reveals peptide dynamics during capture and translocation. *ACS Applied Materials & Interfaces*, *8*(20), 13166–13179.

20. Chavis, A. E., Brady, K. T., Hatmaker, G. A., Angevine, C. E., Kothalawala, N., Dass, A., Robertson, J. W. F., & Reiner, J. E. (2017). Single molecule nanopore spectrometry for peptide detection. *ACS Sensors*, *2*(9), 1319–1328.

21. Tanaka, K., Caaveiro, J. M. M., Morante, K., González-Mañas, J. M., & Tsumoto, K. (2015). Structural basis for self-assembly of a cytolytic pore lined by protein and lipid. *Nature Communications*, *6*, 6337.

22. Huang, G., Willems, K., Soskine, M., Wloka, C., & Maglia, G. (2017). Electro-osmotic capture and ionic discrimination of peptide and protein biomarkers with FraC nanopores. *Nature Communications*, *8*, 935.

23. Huang, G., Voet, A., & Maglia, G. (2019). FraC nanopores with adjustable diameter identify the mass of opposite-charge peptides with 44 dalton resolution. *Nature Communications*, *10*, 835.

24. Iacovache, I., De Carlo, S., Cirauqui, N., Dal Peraro, M., Van Der Goot, F. G, & Zuber, B. (2016). Cryo-EM structure of aerolysin variants reveals a novel protein fold and the pore-formation process. *Nature Communications*, *7*, 12062.

25. Lu, Y., Wu, X. Y., Ying, Y.-L., & Long, Y. T. (2019). Simultaneous single-molecule discrimination of cysteine and homocysteine with a protein nanopore. *Chemical Communications*, *55*(63), 9311–9314.

26. Li, S., Cao, C., Yang, J., & Long, Y. T. (2019). Detection of peptides with different charges and lengths by using the aerolysin nanopore. *Chemelectrochem*, *6*(1), 126–129.

27. Hu, F., Angelov, B., Li, S., Li, Na, Lin, X., & Zou, A. (2020). Single-molecule study of peptides with the same amino acid composition but different sequences by using an aerolysin nanopore. *Chembiochem*, *21*(17), 2467–2473.

28. Piguet, F., Ouldali, H., Pastoriza-Gallego, M., Manivet, P., Pelta, J., & Oukhaled, A. (2018). Identification of single amino acid differences in uniformly charged homopolymeric peptides with aerolysin nanopore. *Nature Communications*, *9*, 966.

29. Ouldali, H., Sarthak, K., Ensslen, T., Piguet, F., Manivet, P., Pelta, J., Behrends, J. C., Aksimentiev, A., & Oukhaled, A. (2020). Electrical recognition of the twenty proteinogenic amino acids using an aerolysin nanopore. *Nature Biotechnology*, *38*, 176–181.

30. Ji, Z., Wang, S., Zhao, Z., Zhou, Z., Haque, F., & Guo, P. (2016). Fingerprinting of peptides with a large channel of bacteriophage phi29 DNA packaging motor. *Small*, *12*(33), 4572–4578.

31. Zhou, Z., Ji, Z., Wang, S., Haque, F., & Guo, P. (2016). Oriented single directional insertion of nanochannel of bacteriophage SPP1 DNA packaging motor into lipid bilayer via polar hydrophobicity. *Biomaterials*, *105*, 222–227.

32. Sun, K., Ju, Y., Chen, C., Zhang, P., Sawyer, E., Luo, Y., & Geng, J. (2020). Single-molecule interaction of peptides with a biological nanopore for identification of protease activity. *Small Methods*, *4*(11), 1900892.

33. Ji, Z., Kang, X., Wang, S., & Guo, P. (2018). Nano-channel of viral DNA packaging motor as single pore to differentiate peptides with single amino acid difference. *Biomaterials*, *182*, 227–233.

34. Ji, Z., & Guo, P. (2019). Channel from bacterial virus T7 DNA packaging motor for the differentiation of peptides composed of a mixture of acidic and basic amino acids. *Biomaterials*, *214*, 119222.

35. Wei, X., Ma, D., Jing, L., Wang, L. Y., Wang, X., Zhang, Z., Lenhart, B. J., Yin, Y., Wang, Q., & Liu, C. (2020). Enabling nanopore technology for sensing individual amino acids by a derivatization strategy. *Journal of Materials Chemistry B*, *8*(31), 6792–6797.

36. Wei, X., Ma, D., Zhang, Z., Wang, L. Y., Gray, J. L., Zhang, L., Zhu, T., Wang, X., Lenhart, B. J., Yin, Y., Wang, Q., & Liu, C. (2020). N-terminal derivatization-assisted identification of individual amino acids using a biological nanopore sensor. *ACS Sensors*, *5*(6), 1707–1716.

37. De Koning-Ward, T. F., Gilson, P. R., Boddey, J. A., Rug, M., Smith, B. J., Papenfuss, A. T., Sanders, P. R., Lundie, R. J., Maier, A. G., Cowman, A. F., & Crabb, B. S. (2009). A newly discovered protein export machine in malaria parasites. *Nature*, *459*, 945–949.

38. Ho, C. - M., Beck, J. R., Lai, M., Cui, Y., Goldberg, D. E., Egea, P. F., & Zhou, Z. H (2018). Malaria parasite translocon structure and mechanism of effector export. *Nature*, *561*, 70–75.

39. Hakamada, K., Watanabe, H., Kawano, R., Noguchi, K., & Yohda, M. (2017). Expression and characterization of the plasmodium translocon of the exported proteins component EXP2. *Biochemical and Biophysical Research Communications*, *482*(4), 700–705.

40. Ohara, M., Takinoue, M., & Kawano, R. (2017). Nanopore logic operation with DNA to RNA transcription in a droplet system. *ACS Synthetic Biology*, *6*(7), 1427–1432.

41. Zhang, H., Hiratani, M., Nagaoka, K., & Kawano, R. (2017). MicroRNA detection at femtomolar concentrations with isothermal amplification and a biological nanopore. *Nanoscale*, *9*(42), 16124–16127.

42. Kisielinska, J., (2013). The exact bootstrap method shown on the example of the mean and variance estimation. *Computational Statistics*, *28*, 1061–1077.

43. Hiratani, M., Ohara, M., & Kawano, R. (2017). Amplification and quantification of an antisense oligonucleotide from target microRNA using programmable DNA and a biological nanopore. *Analytical Chemistry*, *89*(4), 2312–2317.

44. Hiratani, M., & Kawano, R. (2018). DNA logic operation with nanopore decoding to recognize microRNA patterns in small cell lung cancer. *Analytical Chemistry*, *90*(14), 8531–8537.

45. Liu, P., & Kawano, R. (2020). Recognition of single-point mutation using a biological nanopore. *Small Methods*, *4*(11), 2000101.

46. Takiguchi, S., & Kawano, R. (2021). Nanopore decoding for a Hamiltonian path problem. *Nanoscale*, *13*(12), 6192–6200.

47. Sekiya, Y., Sakashita, S., Shimizu, K., Usui, K., & Kawano, R. (2018). Channel current analysis estimates the pore-formation and the penetration of transmembrane peptides. *Analyst*, *143*(15), 3540–3543.

48. Saigo, N., Izumi, K., & Kawano, R. (2019). Electrophysiological analysis of antimicrobial peptides in diverse species. *ACS Omega*, *4*(8), 13124–13130.

49. Sekiya, Y., Shimizu, K., Kitahashi, Y., Ohyama, A., Kawamura, I., & Kawano, R. (2019). Electrophysiological analysis of membrane disruption by bombinin and its isomer using the lipid bilayer system. *ACS Applied Bio Materials*, *2*(4), 1542–1548.

50. Watanabe, H., Gubbiotti, A., Chinappi, M., Takai, N., Tanaka, K., Tsumoto, K., & Kawano, R. (2017). Analysis of pore formation and

protein translocation using large biological nanopores. *Analytical Chemistry*, *89*(21), 11269–11277.

51. Sansom, M. S. P. (1993). Alamethicin and related peptaibols - model ion channels. *European Biophysics Journal with Biophysics Letters*, *22*(2), 105–124.

52. Stoddart, D., Heron, A. J., Klingelhoefer, J., Mikhailova, E., Maglia, G., & Bayley, H. (2010). Nucleobase recognition in ssDNA at the central constriction of the α-hemolysin pore. *Nano Letters*, *10*(9), 3633–3637.

53. Butler, T. Z., Pavlenok, M., Derrington, I. M., Niederweis, M., & Gundlach, J. H. (2008). Single-molecule DNA detection with an engineered MspA protein nanopore. *Proceedings of the National Academy of Sciences of the United States of America*, *105*(52), 20647–20652.

54. Chinappi, M., Yamaji, M., Kawano, R., & Cecconi, F. (2020). Analytical model for particle capture in nanopores elucidates competition among electrophoresis, electroosmosis, and dielectrophoresis. *ACS Nano*, *14*(11), 15816–15828.

55. Fukushima, K., Muraoka, Y., Inoue, T., & Shimozawa, R. (1988). Conformational change of poly (L-lysine) induced by lipid vesicles of dilauroylphosphatidic acid. *Biophysical Chemistry*, *30*(3), 237–244.

56. Reiner, J. E., Kasianowicz, J. J., Nablo, B. J., & Robertson, J. W. F. (2010). Theory for polymer analysis using nanopore-based single-molecule mass spectrometry. *Proceedings of the National Academy of Sciences of the United States of America*, *107*(27), 12080–12085.

SUPPORTING INFORMATION

Additional supporting information may be found online https://doi.org/10.1002/pmic.202100070 in the Supporting Information section at the end of the article.